EPM–RT–2006-06

THREE-DIMENSIONAL MODELING OF CURVED STRUCTURE PARTIALLY OR COMPLETELY CONTAINING AND/OR SUBMERGED IN FLUID

M. Esmailzadeh, A.A. Lakis, M. Thomas et L. Marcouiller
Département de Génie mécanique
École Polytechnique de Montréal
École de technologie Supérieure
Institut de recherche d'Hydro Québec

Juin 2006

Poly

ÉCOLE POLYTECHNIQUE MONTRÉAL

EPM-RT-2006-06

Three-Dimensional Modeling of Curved Structure Partially or Completely Containing and/or Submerged in Fluid

M. Esmailzadeh[1], A.A. Lakis[1], M. Thomas[2] et L. Marcouiller[3]
[1] Département de génie mécanique, École Polytechnique de Montréal
C.P. 6079, succ. Centre Ville Montréal (Québec) H3C 3A7
[2] Département de génie mécanique, École de technologie supérieure
1100, Notre-Dame Ouest, Montréal (Québec) CANADA H3C 1K3
[3] Institut de recherche d'Hydro Québec, Varennes, Québec

Juin 2006

Dépôt légal :
Bibliothèque nationale du Québec, 2006
Bibliothèque nationale du Canada, 2006

EPM-RT-2006-06

Comportement dynamique des plaques rectangulaires submergées

Par : M. Esmailzadeh[1], A.A. Lakis[1], M. Thomas[2] et L. Marcouiller[3]
[1] Département de génie mécanique, École Polytechnique de Montréal
[2] Département de génie mécanique, École de technologie supérieure
[3] Institut de recherche d'Hydro Québec

Abstract

The dynamic behavior of a three-dimensional flexible structure in inviscid incompressible stationary fluid is studied numerically. A hybrid finite element is developed by using classical thin plate theory and finite element analysis, in which the finite elements are rectangular four-noded flat shell, having 5 degrees of freedom per node. The displacement functions are derived from Sanders' thin shell equations. The velocity potential function and Bernoulli's equation for liquid yield an expression for fluid pressure as a function of nodal displacement of the element and inertial force of the quiescent fluid. An analytical integration of the fluid pressure over the element leads to mass matrix of fluid. Calculations are given to illustrate the dynamic behavior of rectangular reservoir containing fluid, as well as a totally submerged blade.

1. Introduction

It is generally known that the natural frequency of a structure in contact with a fluid or immersed in a fluid, decreases significantly compared to the natural frequency of the corresponding dry mode. This problem is referred to as the fluid-structure interaction problem. For this problem, many investigators have suggested some approximate solutions which have been used to predict the changes in the natural frequencies of the structure in the fluid. This is stimulated by new technical applications and also by the availability of powerful numerical tools based on the finite element methods that make numerical solutions of fluid-structure interaction problems possible. However, the use of the finite element method requires enormous amounts of time for modeling and computation. It has been found in subsequent studies that hydrodynamic pressure in a flexible tank can be significantly higher than in the corresponding rigid container due to the interaction effects between flexible walls and contained fluid. Even though there have been numerous studies done on the fluid interaction effects, most of them are concerned with plate and cylindrical tanks. A large number of publications exist on the subject of plate partially or totally immersed in the fluid. Several different approaches have been adopted to describe the fluid actions. Knowledge of the vibration characteristics of rectangular plates submerged in or in contact with fluid is of considerable interest since they are used in many applications, such as the naval, aerospace and construction industries. The hydroelastic behavior of a plate was first described by Lord Rayleigh. Lindholm et al [1] used a strip theory approach and compared the theoretical predictions of resonance frequencies with measured data obtained for a series of cantilevered rectangular plates vibrating in still water. Fu and Price [2] studied the vibration response of cantilevered plates partially or totally immersed in fluid. They used a combination of finite element method and singularity distribution panel approach to examine the effects of the free surface, length and depth of plate on the dynamic characteristics of the plate. Soedel [3] presents an analytical solution for a

simply supported plate, carrying a free surface liquid with reservoir conditions at the edges. Amabili [4] used the Rayleigh-Ritz approach to obtain an analytical solution for the case of fluid domain of fluid depth which either has a free surface or is constrained by rigid walls. Haddara and Cao [5] used the same philosophy to investigate analytically and experimentally dynamic response of submerged plates with various boundary conditions. They provided an analytical added mass factor depending on the height of the free surface and the depth of fluid under plate. The response of shell structures immersed in or conveying flowing fluid has been extensively studied, and general reviews of the literature have been given by Païdoussis [6].Recent books by Païdoussis provide a comprehensive treatment of the subject as well as a complete bibliography of all important work in the field [7,8]. Various elements such as longitudinal and circumferential elements have been developed for closed and open cylindrical [9-15], conical [16] and spherical [17] shells in vacuum or containing a stationary or flowing fluid by Lakis et al. For instance, Lakis and Païdoussis [9] studied the free vibration of a cylindrical shell partially filled with liquid using a combination of finite element method and classical shell theory by employing circumferential element. Lakis and Selmane [18] used longitudinal element to study open cylindrical shell. Lakis and Neagu [19] studied the free surface effects on the dynamics of a cylindrical shell partially filled with liquid. Whilst several well-known finite elements software such as ABAQUS and ANSYS can solve the free vibration of structure in air but they could not correctly predict the natural frequencies of a structure in contact with fluid. Therefore the necessity of an element that could precisely predict natural frequencies of a thin shell subjected to fluid, arises. Very few studies on the dynamic response of rectangular containers exist, but in those studies the flexibility of the structure is not completely taken into account. This may be due to the fact that rectangular fluid containers are usually made of reinforced concrete or may be considered quite rigid. Most of the time, some simplifications have been considered, which lead us to treat a 3D structure as 2D modeling. Kim et

al [20] presented analytic solution to study dynamic behavior of a rectangular reservoir partially filled with fluid using the Rayleigh-Ritz method. However in their study, only a pair of walls is assumed to be flexible while the other pair and bottom remain rigid, as if they studied two parallel plates. Kim and Lee [21] investigated hydroelastic analysis of a rectangular tank completely filled with liquid by using NASTRAN program and compared results with analytic solution, however they considered tank as two parallel plates because of rigid bottom and two parallel walls. Jeong and Lee [22] developed an analytic method to estimate the natural frequencies of two identical rectangular plates by using a finite Fourier series expansion method. It is assumed that an ideal fluid is surrounded by the plates and a rigid rectangular container. Their theoretical results are compared with finite element method by ANSYS software. Bauer and Eidel [23] investigated researches on a two-dimensional rectangular container of infinite width partially covered with an elastic plate (beam) and partially filled with fluid. The present study seems to be the first one on the dynamics behavior of three dimensional shell structures in vacuo and subjecting to the quiescent fluid. This paper introduces a general approach to the dynamic analysis of a thin, elastic, isotropic three-dimensional shell in air as well as subjecting to fluid. The method is a hybrid of finite element theory and classical thin plate theory. The displacement functions are derived from Sanders' thin shell equations, and are expanded in power series. Expressions for mass and stiffness are determined by precise analytical integration. Linear potential flow theory is applied to describe the fluid-structure interaction; in fact, the amplitude of shell displacements remains small enough for linear fluid mechanics to be adequate. In the present work, we intend to develop an element, to be able to model any 3D thin structure, such as hydraulic turbine blade or completely flexible rectangular reservoir. An empty and fluid-filled rectangular reservoir under different boundary conditions has been studied. In order to demonstrate the applicability of the proposed method a submerged turbine blade is investigated, as well. The purpose of the present paper is to present a

more accurate and general numerical analysis using a rectangular shell element [24]. The method used here has been employed successfully for various structures, such as rectangular reservoir or blade. The obtained results have been compared by ANSYS and accuracy of the proposed numerical method has been verified.

2. Fundamental Equation

2.1. Equation of motion and displacement functions

A rectangular flat shell element having four nodes, each of which has five degrees of freedom as shown in Fig. 1 has been used as a finite element.

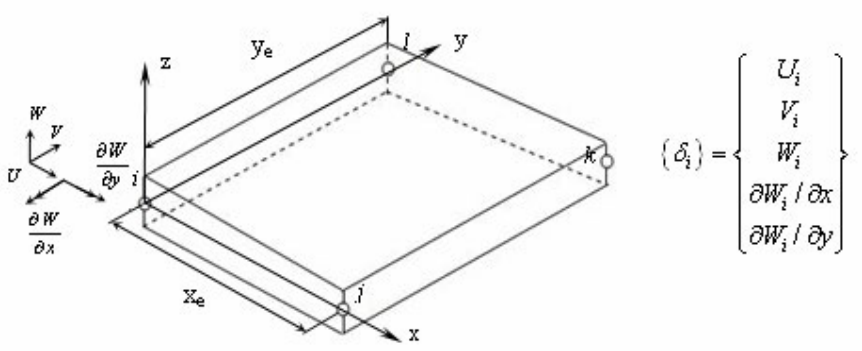

Fig. 1: Flat rectangular shell element

To establish the equilibrium equations of the plate, we use Sanders' equations for cylindrical shells and assume the radius of the shell to be infinite. The three equations take into account both membrane and bending effects. Sanders based his equations on Love's first approximation for thin shell, and showed that all strains vanish for any rigid-body motion. This shell's theory satisfies the convergence criteria for small rigid-body motions. The equilibrium equations of an orthotropic plate in terms of the in-plane and normal displacements of the plate mean surface are written as:

$$P_{22}\frac{\partial^2 V}{\partial y^2}+P_{21}\frac{\partial^2 U}{\partial x\,\partial y}+P_{33}\left(\frac{\partial^2 U}{\partial x\,\partial y}+\frac{\partial^2 V}{\partial x^2}\right)=0$$

$$P_{11}\frac{\partial^2 U}{\partial y^2}+P_{12}\frac{\partial^2 V}{\partial x\,\partial y}+P_{33}\left(\frac{\partial^2 V}{\partial x\,\partial y}+\frac{\partial^2 U}{\partial y^2}\right)=0$$

$$P_{44}\frac{\partial^4 W}{\partial x^4}+(P_{45}+P_{54}+2P_{66})\frac{\partial^4 W}{\partial x^2\,\partial y^2}+P_{55}\frac{\partial^4 W}{\partial y^4}=0 \tag{1}$$

P_{ij} are the terms of elasticity matrix [25].

The first two equations describe the membrane behavior and the third equation specifies the bending of a rectangular plate. In this case, the equations of motion are decoupled. Unfortunately, the exact solution of the equations of motion is very complicated in the case of plate. To surmount this problem, we assume the solution of membrane displacements to be bilinear polynomial and the normal displacement will be determined from plate's equation of motion [24]. Therefore, the displacement functions will be written as follows:

$$U(x,y,t)=C_1+C_2\frac{x}{A}+C_3\frac{y}{B}+C_4\frac{xy}{AB} \tag{2}$$

$$V(x,y,t)=C_5+C_6\frac{x}{A}+C_7\frac{y}{B}+C_8\frac{xy}{AB} \tag{3}$$

$$W(x,y,t)=\sum_{j=9}^{20}C_j e^{i\pi\left(\frac{x}{A}+\frac{y}{B}\right)+i\omega t} \tag{4}$$

where A and B are the plate length and width in x and y directions, respectively[24].

We could expand the exponential solution of normal deflection, W in Taylor series as follows:

$$\begin{aligned}W(x,y,t)=C_9+C_{10}\frac{x}{A}+C_{11}\frac{y}{B}+C_{12}\frac{x^2}{2A^2}+C_{13}\frac{xy}{AB}+C_{14}\frac{y^2}{2B^2}+C_{15}\frac{x^3}{6A^3}+C_{16}\frac{x^2y}{2A^2B}\\+C_{17}\frac{xy^2}{2AB^2}+C_{18}\frac{y^3}{6B^3}+C_{19}\frac{x^3y}{6A^3B}+C_{20}\frac{xy^3}{6AB^3}\end{aligned} \tag{5}$$

We can rewrite the displacements U, V and W in matrix form,

$$\begin{Bmatrix} U \\ V \\ W \end{Bmatrix} = [R]\{C\} \tag{6}$$

where [*R*] is a 3×20 matrix, in which the components are in terms of *x* and *y* [24]. The vector $\{C\}$ is given by

$$\{C\} = \{C_1, C_2, ..., C_{20}\}^T \tag{7}$$

In which its components are generalized coordinates.

To determine these constants we need 20 boundary conditions, which are 5 degrees of freedom per node of a rectangular element. The nodal degrees of freedom consist of translations along the Cartesian directions x, y and z and the rotations about two in-plane axes. The nodal displacement vector of an element is:

$$\{\delta\} = \{\delta_i, \delta_j, \delta_k, \delta_l\}^T \tag{8}$$

And the nodal displacement of each node is:

$$\{\delta_i\} = \left\{U_i, V_i, W_i, \frac{\partial W_i}{\partial x}, \frac{\partial W_i}{\partial y}\right\}^T \tag{9}$$

where $U_i, V_i, W_i, \frac{\partial W_i}{\partial x}, \frac{\partial W_i}{\partial y}$ are in-plane displacements, normal deflection of the mean surface and rotations about the plane axes, corresponding to node *i*, respectively. The nodal displacement vector of each element could be obtained as:

$$\{\delta\} = [A]\{C\} \tag{10}$$

By substituting $\{C\}$ from (10) into (6):

$$\begin{Bmatrix} U \\ V \\ W \end{Bmatrix} = [R][A]^{-1}\{\delta\} = [N]\{\delta\} \tag{11}$$

where [*N*] is the shape function of the rectangular plate element and $[A]^{-1}$ is given in [24].

2.2. Kinematics relationship

Strain vector in terms of displacements is given by:

$$\{\varepsilon\}=\begin{Bmatrix}\varepsilon_x\\ \varepsilon_y\\ 2\varepsilon_{xy}\\ \kappa_x\\ \kappa_y\\ 2\kappa_{xy}\end{Bmatrix}=\begin{Bmatrix}\partial U/\partial x\\ \partial V/\partial y\\ \partial U/\partial y+\partial V/\partial x\\ -\partial^2 W/\partial x^2\\ -\partial^2 W/\partial y^2\\ -\partial^2 W/\partial x\partial y\end{Bmatrix} \tag{12}$$

By substituting the displacements from Eq. (11) into Eq. (12), we obtain strain vector in terms of nodal displacements.

$$\{\varepsilon\}=[D][R][A]^{-1}\{\delta\}=[Q][A]^{-1}\{\delta\}=[B]\{\delta\} \tag{13}$$

where [Q] is 5×20 matrix [24].

2.3. Stress strain relationship

We can define stress vector,

$$\{\sigma\}=[P]\{\varepsilon\} \tag{14}$$

By introducing Eq. (13) into (14), stress vector is obtained by:

$$\{\sigma\}=[P][B]\{\delta\} \tag{15}$$

The rigidity and mass matrices of each rectangular element can be written:

$$[K]_e=\int_0^{x_e}\int_0^{y_e}[B]^T[P][B]dA \tag{16}$$

$$[M]_e=\rho_s h\int_0^{x_e}\int_0^{y_e}[N]^T[N]dA \tag{17}$$

where, x_e and y_e are the dimensions of the element in x and y coordinates and ρ_s is the density of shell, h its thickness and dA a surface element. By substituting [B] and [N] into Eqs. (16) and (17), we obtain,

$$[K]_e = \left[[A]^{-1}\right]^T \left(\int_0^{x_e} \int_0^{y_e} [Q]^T [P][Q] dxdy \right) [A]^{-1} \tag{18}$$

$$[M]_e = \left[[A]^{-1}\right]^T \left(\rho_s h \int_0^{x_e} \int_0^{y_e} [R]^T [R] dxdy \right) [A]^{-1} \tag{19}$$

The matrices $[M]_e$ and $[K]_e$ were obtained analytically by carrying out the necessary matrix operations and integration over x and y.

$$[K]_e = \left[[A]^{-1}\right]^T [G][A]^{-1} \tag{20}$$

$$[M]_e = \rho_s h \left[[A]^{-1}\right]^T [S][A]^{-1} \tag{21}$$

The development of the shell elements from the classical shell theory is more complex and many approximations are required to simplify the solution whereas flat shell elements are easier to formulate using previously available theories of membrane and plate bending elements. Flat shell elements are developed by superimposing the stiffness of membrane and bending elements. The membrane and bending forces are totally independent of each other in the flat shell elements and hence there is no membrane-bending coupling present in the element itself. This is major advantage of the flat shell elements. This separation is no longer possible in folded plates or curved shells. The behavior of a continuously curved surface can be adequately represented by the behavior of a surface built up of small flat elements. The shell is subdivided into rectangular finite elements. The transformation between global and local coordinates is required to generate the element global stiffness matrix and to write the appropriate equilibrium equations. The local-global transformation increases the number of the degree of freedom. This is a consequence of the absence of the rotational stiffness about the local axis. This can cause singularity and an error in the most equation

solvers. Since there is no stiffness associated with 6th degree of freedom, i.e. normal rotation, therefore singularity arises. For surmounting singularity problem, three ways are proposed; the first approach is to insert a fictitious stiffness associated with the local rotation in local coordinates, the second approach is to eliminate the 6th degree of freedom for all co-planar nodes and the last approach is to define the 6th degree of freedom in terms of U and V as $\theta_z = \frac{1}{2}(\frac{\partial U}{\partial y} - \frac{\partial V}{\partial x})$. The most common approach is to insert a weak fictitious rigidity associated with the local normal rotation. The nodal displacement defined in the local shell element contain only two rotation components, the third rotation about the normal axis does not appear in the strain definition and is therefore not required to model the structure behavior of each individual element. Classical shell equations do not produce equations associated with this rotational parameter. However, when several elements meeting at a common node lie in different planes, it is necessary to include the rotation about the normal, θ_z for a consistent transformation of displacements from the local to global coordinate system. To define coordinate transformation matrix of element, two ways are suggested; either using two successive rotations about x and y axes or using direction cosine. Transformation matrix characterized by two successive rotations $[R_x]$ and $[R_y]$ are defined as follows:

$$\{\delta\}_{Global} = [T]\{\delta\}_{Local} \tag{22}$$

$$[T]_{node} = [R_x(\beta)][R_y(\alpha)] \tag{23}$$

$$[R_x] = \begin{bmatrix} 1 & 0 & 0 & 0 & 0 & 0 \\ 0 & \cos\beta & -\sin\beta & 0 & 0 & 0 \\ 0 & \sin\beta & \cos\beta & 0 & 0 & 0 \\ 0 & 0 & 0 & \cos\beta & 0 & \sin\beta \\ 0 & 0 & 0 & 0 & 1 & 0 \\ 0 & 0 & 0 & -\sin\beta & 0 & \cos\beta \end{bmatrix} \tag{24}$$

$$\left[R_y\right]=\begin{bmatrix} \cos\alpha & 0 & \sin\alpha & 0 & 0 & 0 \\ 0 & 1 & 0 & 0 & 0 & 0 \\ -\sin\alpha & 0 & \cos\beta & 0 & 0 & 0 \\ 0 & 0 & 0 & 1 & 0 & 0 \\ 0 & 0 & 0 & 0 & \cos\alpha & \sin\alpha \\ 0 & 0 & 0 & 0 & -\sin\alpha & \cos\alpha \end{bmatrix} \tag{25}$$

Transformation matrix could be also defined by vector algebra using direction cosines between the two sets of axes of a rectangular element. The vector passing through nodes 1 and 2 is given by,

$$V_x = \begin{Bmatrix} x_2 - x_1 \\ y_2 - y_1 \\ z_2 - z_1 \end{Bmatrix} \tag{26}$$

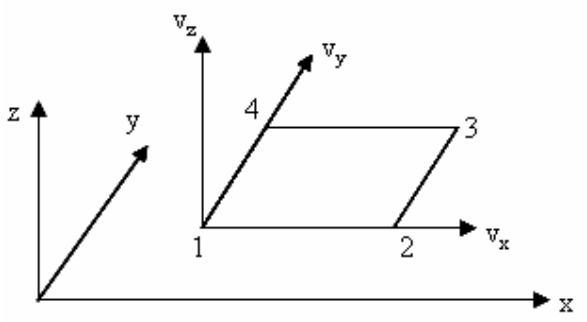

Fig. 2: Coordinate transformation for rectangular element

where *x, y* and *z* represent the global coordinates of node. The direction cosine for the local x direction is obtained by normalizing the vector with respect to its length.

$$\Lambda_x = \frac{1}{l_{21}} \begin{Bmatrix} x_2 - x_1 \\ y_2 - y_1 \\ z_2 - z_1 \end{Bmatrix} \tag{27}$$

where $l_{21} = \sqrt{(x_2 - x_1)^2 + (y_2 - y_1)^2 + (z_2 - z_1)^2}$ is the length of vector.

The direction cosines of the y-axis are established in a similar manner,

$$\Lambda_y = \frac{1}{l_{41}}\{V_y\} = \frac{1}{l_{41}}\begin{Bmatrix} x_4 - x_1 \\ y_4 - y_1 \\ z_4 - z_1 \end{Bmatrix} \tag{28}$$

where $l_{41} = \sqrt{(x_4 - x_1)^2 + (y_4 - y_1)^2 + (z_4 - z_1)^2}$ is the length of vector V_y. The direction cosine normal to the plane that represents the element local z direction is obtained by the cross product of direction cosines Λ_x and Λ_y.

$$\Lambda_z = \Lambda_x \times \Lambda_y \tag{29}$$

The transformation matrix between two sets of axes is expressed by

$$[xyz]_{Global} = [\Lambda][\overline{xyz}]_{Local} \tag{30}$$

$$\Lambda = \left[\{\Lambda_x\}_{3\times1} \quad \{\Lambda_y\}_{3\times1} \quad \{\Lambda_z\}_{3\times1}\right] = \begin{bmatrix} \Lambda_{\bar{x}x} & \Lambda_{\bar{y}x} & \Lambda_{\bar{z}x} \\ \Lambda_{\bar{x}y} & \Lambda_{\bar{y}y} & \Lambda_{\bar{z}y} \\ \Lambda_{\bar{x}z} & \Lambda_{\bar{y}z} & \Lambda_{\bar{z}z} \end{bmatrix} = \begin{bmatrix} \cos(\bar{x},x) & \cos(\bar{y},x) & \cos(\bar{z},x) \\ \cos(\bar{x},y) & \cos(\bar{y},y) & \cos(\bar{z},y) \\ \cos(\bar{x},z) & \cos(\bar{y},z) & \cos(\bar{z},z) \end{bmatrix} \tag{31}$$

In general, transformation matrix of a node is defined by (22) and consequently, by using direction cosine we have,

$$\{U \quad V \quad W \quad \theta_x \quad \theta_y \quad \theta_z\}^T_{Global} = \begin{bmatrix} [\Lambda] & 0 \\ 0 & [\Lambda] \end{bmatrix}\{U \quad V \quad W \quad \theta_x \quad \theta_y \quad \theta_z\}^T_{Local} \tag{32}$$

Rotations about in-plane axes for a thin flat rectangular shell element are expressed:

$$\theta_x = \partial W / \partial y \quad , \quad \theta_y = -\partial W / \partial x \tag{33}$$

Therefore the transformation matrix for nodal displacement becomes:

$$\left\{U \quad V \quad W \quad \frac{\partial W}{\partial x} \quad \frac{\partial W}{\partial y} \quad \theta_z\right\}^T_{Global} = [T]\left\{U \quad V \quad W \quad \frac{\partial W}{\partial x} \quad \frac{\partial W}{\partial y} \quad \theta_z\right\}^T_{Local} \tag{34}$$

The nodal transformation matrix made up of the direction cosines is expressed by,

$$[T]=\begin{bmatrix} \Lambda_{\bar{x}x} & \Lambda_{\bar{y}x} & \Lambda_{\bar{z}x} & 0 & 0 & 0 \\ \Lambda_{\bar{x}y} & \Lambda_{\bar{y}y} & \Lambda_{\bar{z}y} & 0 & 0 & 0 \\ \Lambda_{\bar{x}z} & \Lambda_{\bar{y}z} & \Lambda_{\bar{z}z} & 0 & 0 & 0 \\ 0 & 0 & 0 & \Lambda_{\bar{y}y} & -\Lambda_{\bar{x}y} & -\Lambda_{\bar{z}y} \\ 0 & 0 & 0 & -\Lambda_{\bar{y}x} & \Lambda_{\bar{x}x} & \Lambda_{\bar{z}x} \\ 0 & 0 & 0 & -\Lambda_{\bar{y}z} & \Lambda_{\bar{x}z} & \Lambda_{\bar{z}z} \end{bmatrix} \tag{35}$$

The transformation matrix for rectangular shell element is,

$$[T]_{element}=\begin{bmatrix} [T] & 0 & 0 & 0 \\ 0 & [T] & 0 & 0 \\ 0 & 0 & [T] & 0 \\ 0 & 0 & 0 & [T] \end{bmatrix} \tag{36}$$

Stiffness and mass matrices of an element in the global coordinates could be computed as,

$$[K]_{Global} = [T][K]_{Local}[T]^T \tag{37}$$

$$[M]_{Global} = [T][M]_{Local}[T]^T \tag{38}$$

Once the stiffness and the mass matrices have been obtained, it is possible to construct the global matrices for the complete structure using the finite element assembly technique.

In the case of free vibration, the equations of motion are

$$[M_s]\{\ddot{\delta}\}+[K_s]\{\delta\}=0 \tag{39}$$

3. Behavior of Fluid solid interaction

The dynamic behavior of a shell subjected to flowing fluid can be represented by the following system:

$$[[M_s]-[M_f]]\{\ddot{\delta}\}-[C_f]\{\dot{\delta}\}+[[K_s]-[K_f]]\{\delta\}=\{0\} \tag{40}$$

where $\{\delta\}$ is displacement vector, [M_s], [K_s] are respectively the mass and stiffness matrices of the system in vacuo; [M_f], [C_f] and [K_f] represent the inertial, Coriolis and centrifugal forces which are induced by potential flow, respectively. As a structure vibrates in a fluid at rest, the fluid is set into

motion and couples its motion with that of the structure during vibration. As a consequence the fluid contributes its own stiffness and mass to that of structure. The stiffness of a quiescent fluid is negligible whereas the mass of fluid is added to the structure and reduces the natural frequency of the system. In other words, the natural frequencies of structures which are in contact with fluid, decrease substantially compared to natural frequencies in vacuo, due to increasing of kinetic energy of the total system.

The dynamic behavior of a rectangular shell element subjected to a stationary fluid can be represented by the following system,

$$\left[\left[M_s\right]-\left[M_f\right]\right]\left\{\ddot{\delta}\right\}+\left[K_s\right]\left\{\delta\right\}=0 \tag{41}$$

The inertial force of the stationary fluid is taken into account as mass matrix of the fluid.

Potential flow is an idealized method of modeling flow. In mathematical model, the fluid is assumed inviscid, incompressible and its motion is irrotational and its mean velocity distribution is constant across shell section. We suppose that shell displacements remain small enough for linear fluid mechanics to be adequate. Velocity potential function, φ must satisfy the Laplace equation throughout the fluid domain. This relation is expressed in Cartesian coordinate system by

$$\nabla^2\phi=\frac{\partial^2\phi}{\partial x^2}+\frac{\partial^2\phi}{\partial y^2}+\frac{\partial^2\phi}{\partial z^2}=0 \tag{42}$$

where *x, y* and *z* are in-plane and normal directions of a plate, respectively.

A fluid velocity vector can be expressed as gradient of the velocity potential function as,

$$V(x,y,z,t)=\nabla\phi(x,y,z,t) \tag{43}$$

$$V_x=U_x+\frac{\partial\phi}{\partial x}\ ,\ V_y=\frac{\partial\phi}{\partial y}\ ,\ V_z=\frac{\partial\phi}{\partial z} \tag{44}$$

where U_x is the unperturbed flow velocity along shell in the x-direction. The remaining components of velocity, V_x, V_y and V_z are disturbance or perturbation fluid velocity in three directions.

The dynamic condition on fluid-shell surfaces can be determined by the Bernoulli equation:

$$\frac{\partial \phi}{\partial t} + \frac{1}{2} V^2 + \frac{P}{\rho_f} = 0 \tag{45}$$

where ρ_f is the density of fluid. Upon introducing velocity into above equation and taking into account only the linear terms (neglecting the higher order terms), the Bernoulli equation at the wall of shell element is expressed by,

$$\frac{\partial \phi}{\partial t} + U_x \frac{\partial \phi}{\partial x} + \frac{P}{\rho_f} = 0 \tag{46}$$

Therefore hydrodynamic pressure on the fluid-shell surface for a stationary fluid ($U_x=0$) is obtained by,

$$P\Big|_{at\ the\ wall} = -\rho_f \frac{\partial \phi}{\partial t} \tag{47}$$

A full definition of the flow requires that a condition be applied to the structure-fluid interface. At the interface, the impermeability condition can be written as follows:

$$V_z\Big|_{at\ the\ wall} = U_x \frac{\partial W}{\partial x} + \frac{\partial W}{\partial t} \tag{48}$$

Since $U_x=0$ and $V_z = \frac{\partial \phi}{\partial z}$, therefore the impermeability condition could be written as,

$$\frac{\partial \phi}{\partial z}\Big|_{at\ the\ wall} = \frac{\partial W}{\partial t} \tag{49}$$

$$\frac{\partial \phi}{\partial z}\Big|_{z=0} = \frac{\partial W}{\partial t} \tag{50}$$

$$\frac{\partial \phi}{\partial z}\Big|_{z=-h} = \frac{\partial W}{\partial t} \tag{51}$$

where W is the lateral displacement of the shell element.

The velocity potential function could be expressed into two separate functions:

$$\phi(x,y,z,t) = F(z)S(x,y,t) \tag{52}$$

By introducing (52) into (49) and then by substituting *S(x,y,t)* into (52) the velocity potential function can be expressed:

$$\phi(x,y,z,t) = \frac{F(z)}{F'(0)}\frac{\partial W}{\partial t} \tag{53}$$

$$\phi(x,y,z,t) = \frac{F(z)}{F'(-h)}\frac{\partial W}{\partial t} \tag{54}$$

By substituting φ into Bernoulli equation we obtain pressure at both sides of shell element:

$$P\big|_{z=0} = -\rho_f \frac{F(0)}{F'(0)}\frac{\partial^2 W}{\partial t^2} \tag{55}$$

$$P\big|_{z=-h} = -\rho_f \frac{F(-h)}{F'(-h)}\frac{\partial^2 W}{\partial t^2} \tag{56}$$

Therefore total pressure imposing on shell element from fluid can be expressed by:

$$P_{total} = -\rho_f \left(\frac{F(0)}{F'(0)} - \frac{F(-h)}{F'(-h)}\right)\frac{\partial^2 W}{\partial t^2} = -\rho_f Z_f \ddot{W} \tag{57}$$

Substituting *W* from Eq. (4) into Eqs. (53) and (54) and then introducing φ into Laplace equation yields the following equation:

$$\frac{\partial^2 F(z)}{\partial z^2} - \pi^2\left(\frac{1}{A^2} + \frac{1}{B^2}\right)F(z) = 0 \tag{58}$$

The general solution of $F'' - \mu^2 F = 0$ is

$$F(z) = A_1 e^{\mu z} + A_2 e^{-\mu z} \tag{59}$$

$$\mu^2 = \pi^2\left(\frac{1}{A^2} + \frac{1}{B^2}\right) \tag{60}$$

By introducing *F(z)* into Eqs. (53) and (54) the velocity potential function is obtained:

$$\phi(x,y,z,t) = \left(\frac{A_1 e^{\mu z} + A_2 e^{-\mu z}}{F'(0)}\right)\frac{\partial W}{\partial t} \tag{61}$$

$$\phi(x,y,z,t)=\left(\frac{A_1e^{\mu z}+A_2e^{-\mu z}}{F'(-h)}\right)\frac{\partial W}{\partial t} \tag{62}$$

Velocity potential function, φ, must satisfy the boundary conditions at the fluid-solid interaction and boundary conditions of fluid. One should take note that boundary conditions could vary from one case to another, therefore one should prescribe boundary conditions precisely. In general, three boundary conditions exist; fluid free surface, rigid wall, i.e., $\frac{\partial\phi}{\partial z}\big|_{z=h_1}=0$ and impermeability. To obtain an overall understanding of the problem, we have studied a completely flexible rectangular reservoir containing fluid. The following conditions should be considered:

3.1. Fluid over a plate with free surface condition

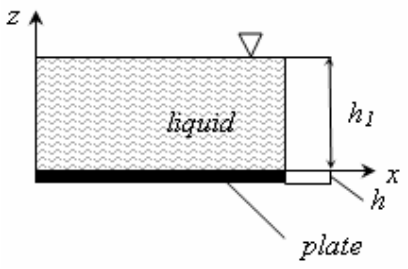

Fig. 3: Fluid solid element having free surface at $z=h_1$

Consider fluid over a plate. At the interface, the impermeability condition is:

$$\frac{\partial\phi}{\partial z}\big|_{z=0}=\frac{\partial W}{\partial t} \tag{63}$$

The free surface behavior is expressed by [26]:

$$\frac{\partial\phi}{\partial z}\big|_{z=h_1}=-\frac{1}{g}\frac{\partial^2\phi}{\partial t^2} \tag{64}$$

where g is gravitational acceleration.

By substituting boundary conditions (63) and (64) into Eq. (61):

$$\frac{F(0)}{F'(0)} = \frac{1 + C_1 e^{2\mu h_1}}{\mu(1 - C_1 e^{2\mu h_1})} \tag{65}$$

where C_1 is defined as following, in which μ is obtained by Eq. (60). C_1 approximately tends to -1,

$$C_1 = \frac{\mu g - \omega^2}{\mu g + \omega^2} \tag{66}$$

By introducing $\frac{F(0)}{F'(0)}$ from (65) into Eq. (57), the fluid pressure applying on the bottom plate of a reservoir is obtained by:

$$P_{total} = -\rho_f \left(\frac{1 + C_1 e^{2\mu h_1}}{\mu(1 - C_1 e^{2\mu h_1})} \right) \frac{\partial^2 W}{\partial t^2} \tag{67}$$

$$Z_f = \frac{1 + C_1 e^{2\mu h_1}}{\mu(1 - C_1 e^{2\mu h_1})} \tag{68}$$

3. 2. Fluid bounded between two parallel plates

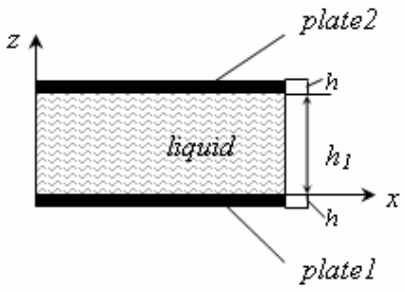

Fig. 4: Two identical plates coupled with bounded fluid

Boundary conditions for both plates at $z=0$ and $z=h_1$ are defined by impermeability condition:

$$\frac{\partial \phi}{\partial z}\Big|_{z=0} = \frac{\partial W}{\partial t} \quad , \quad \frac{\partial \phi}{\partial z}\Big|_{z=h_1} = \frac{\partial W}{\partial t} \tag{69}$$

By introducing these boundary conditions into Eq. (61):

$$\frac{F(0)}{F'(0)} = \frac{1-2e^{\mu h_1}+e^{2\mu h_1}}{\mu(1-e^{2\mu h_1})} \tag{70}$$

By introducing $\frac{F(0)}{F'(0)}$ into Eq. (57) the fluid pressure applying on each wall is obtained by:

$$P_{total} = -\rho_f \left(\frac{1-2e^{\mu h_1}+e^{2\mu h_1}}{\mu(1-e^{2\mu h_1})} \right) \frac{\partial^2 W}{\partial t^2} \tag{71}$$

$$Z_f = \frac{1-2e^{\mu h_1}+e^{2\mu h_1}}{\mu(1-e^{2\mu h_1})} \tag{72}$$

Fluid mass matrix could be obtained by performing the following integration,

$$\{F\} = \int_A [N]^T \begin{Bmatrix} 0 \\ 0 \\ -P_{total} \end{Bmatrix} dA = \int_A [N]^T \begin{Bmatrix} 0 \\ 0 \\ \rho_f Z_f \ddot{W} \end{Bmatrix} dA = [M_f] \{\ddot{\delta}\} \tag{73}$$

This leads us to added mass,

$$[M_f] = \rho_f Z_f \left[[A]^{-1} \right]^T [S_f] [A]^{-1} \tag{74}$$

$$S_f = \int_0^{x_e} \int_0^{y_e} [R]^T [R_f] dx\, dy \tag{75}$$

Where $[R_f]$ is given in [24].

4. Calculations and discussions

4.1. Fluid-filled reservoir

On the basis of the preceding analysis, natural frequencies of a rectangular reservoir in vacuo, completely and partially filled with fluid are calculated by using in-house program. Consider a lidless rectangular tank consisting of side walls and bottom, whose geometry is depicted in Fig. 5, where the properties are; the Young's modulus $E = 2 \times 10^{11}$ Pa, the Poisson's ratio $\nu = 0.3$, the thickness $h = 0.005$ m and the density $\rho_s = 7970$ kg/m^3. Water is used as the containing fluid having a density of $\rho_f = 1000$ kg/m^3. Two cases of boundary conditions have been studied: a) the bottom and facing walls of the reservoir are considered to be simply supported at edges and b) the bottom is clamped.

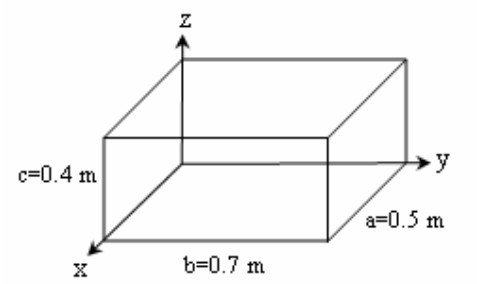

Fig. 5: A rectangular reservoir

In order to check the validity of the calculations, a finite element analysis was carried out using ANSYS. As mentioned before, in our theory, we have total compatibility between the solid and the fluid elements, whereas in ANSYS two separate elements are used as fluid and solid elements. The three dimensional model consists of 3D contained fluid elements (FLUID80) and elastic shell elements (SHELL63). The reservoir is discretized with four-noded quadrilateral shell elements, which have both bending and membrane capabilities. It has six degrees of freedom at each node; translations in three directions and rotations about three axes. FLUID80 element is used to model

fluid contained within vessels having no flow rate. The fluid element is defined by eight nodes having three translations in each direction and the isotropic material properties. Fluid has to be considered as compressible. Fluid elastic modulus should be the bulk modulus of fluid, approximately 3×10^5 psi for water. In ANSYS the impermeability condition is not respected. Fluid element at a boundary should not be attached directly to structural elements but should have separate, coincident nodes that are coupled only in the direction normal to the interface. The reservoir is meshed and divided into 131 elastic shell elements and the fluid region consists of 140 fluid elements with connectivity to the plate elements.

The first few natural frequencies of the empty and fluid-filled simply supported rectangular reservoir are listed and compared with the ANSYS results in Tables 1 and 2 (case a). Tables 3 and 4 present the natural frequencies of the empty and fluid-filled bottom-clamped rectangular reservoir, respectively (case b).

Table.1: Comparison of present element and ANSYS for the empty reservoir, simply supported at all edges (case a)

Natural Frequency (Hz)		
ANSYS	Present	Discrepancy
91.618	91	0.006745399
119.11	118.3	0.006800437
128.01	127.5	0.003984064
143.97	142.4	0.01090505
157.61	156	0.010215088
174.21	172.4	0.010389759
193.92	190.9	0.015573432
213.18	210.4	0.013040623

Table.2: Comparison of present element and ANSYS for the fluid-filled reservoir, simply supported at all edges (case a)

Coupled Natural Frequency (Hz)		
ANSYS	Present element	Discrepancy
38.994	44.92	0.131923419
53.237	61.24	0.13068256
57.511	65.8	0.125972644
70.988	74.63	0.04880075
72.496	82.46	0.120834344
85.515	86.13	0.007140369
100.96	99.08	0.018974566
101.66	108.5	0.063041475

Table.3: Comparison of present element and ANSYS for the empty bottom-clamped rectangular reservoir (case b)

Natural Frequency (Hz)		
ANSYS	Present element	Discrepancy
53.44	52.98	0.008607784
59.676	59.12	0.009316978
85.982	85.08	0.010490568
100.34	99.48	0.008570859
136.19	134.9	0.009472061
153.56	152.6	0.006251628
195.64	194.9	0.003782458
197.25	196.2	0.005323194

Table.4: Comparison of present element and ANSYS for fluid-filled bottom-clamped rectangular reservoir (case b)

Coupled Natural Frequency (Hz)		
ANSYS	Present element	Discrepancy
26.519	27.61	0.039514669
29.917	30.69	0.025187357
45.05	45.3	0.005518764
45.32	52.98	0.144582861
73.309	70.15	0.045032074
74.676	79.61	0.061977139
90.995	101.2	0.100839921
95.278	101.8	0.064066798

4.2. Partially-filled reservoir

Variation of natural frequencies as a function of fluid level variations under different boundary conditions for an open reservoir has been investigated and depicted in Figs. 6-12, in which the frequencies have been denoted as; —◆— 1st, —■— 2nd and —▲— 3rd frequencies. In these figures natural frequencies of the system as a function of fluid level have been shown. As we mentioned earlier, the stiffness of a quiescent fluid is negligible in fluid-solid analysis whereas the mass of fluid is added to the structure and reduces the natural frequency, due to increasing of kinetic energy of total system.

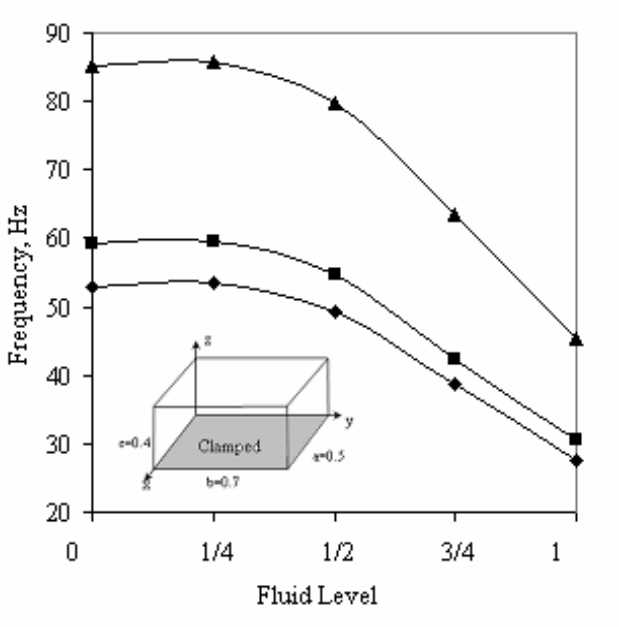

Fig. 6: Variation of frequencies of bottom-clamped reservoir versus fluid level variations

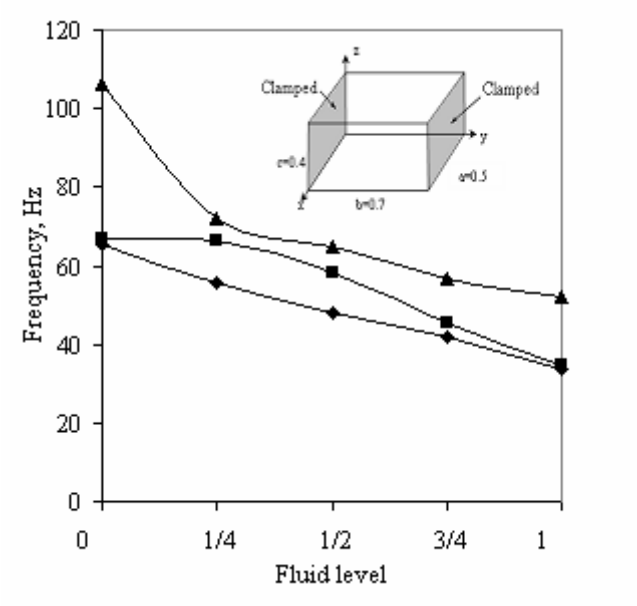

Fig. 7: Variation of frequencies of reservoir with two parallel clamped walls versus fluid level variations

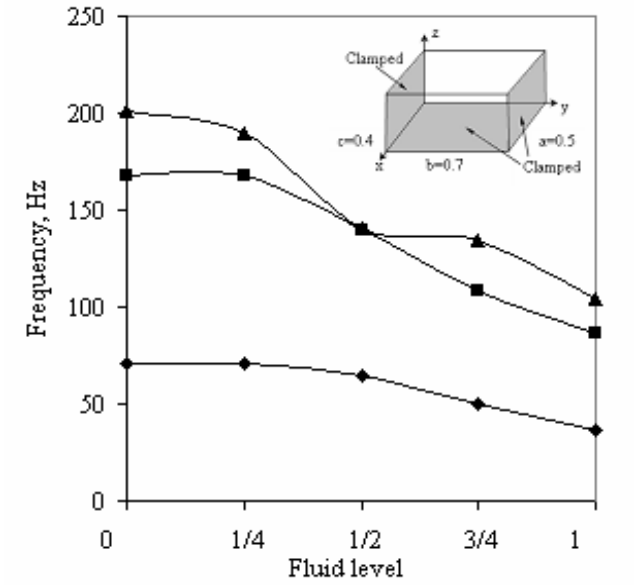

Fig. 8: Variation of frequencies of reservoir with two facing walls and bottom clamped versus fluid level variations

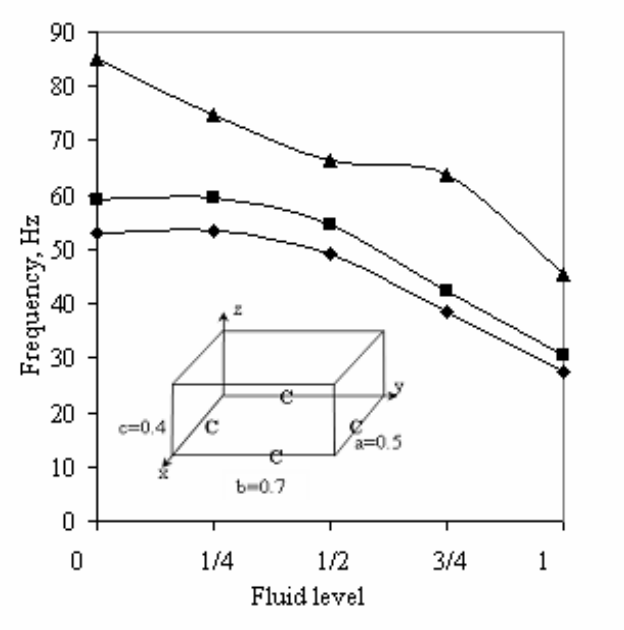

Fig. 9: Variation of frequencies of a perimetrically bottom clamped rectangular reservoir versus fluid level variations

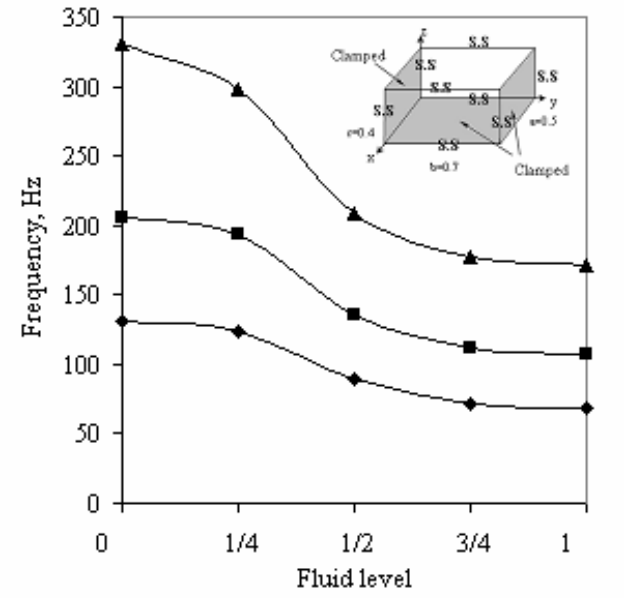

Fig. 10: Variation of frequencies of a reservoir with two facing walls and bottom clamped and two other walls simply supported at edges versus fluid level variations

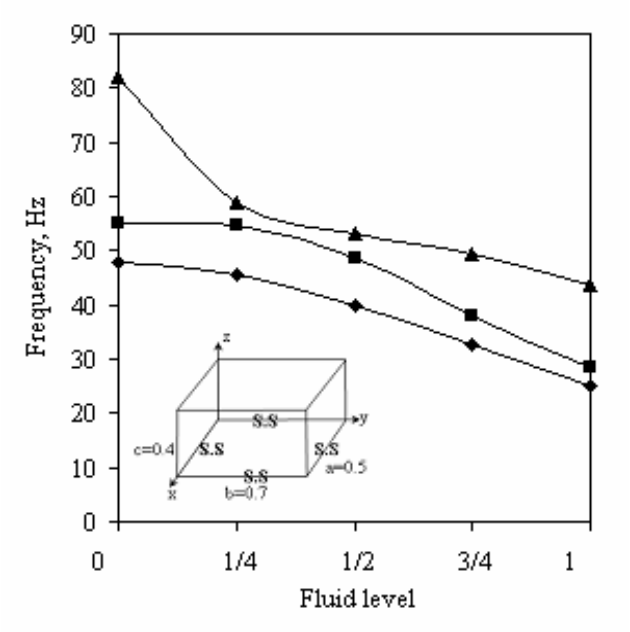

Fig. 11: Variation of frequencies of a perimetrically simply supported bottom reservoir versus fluid level variation

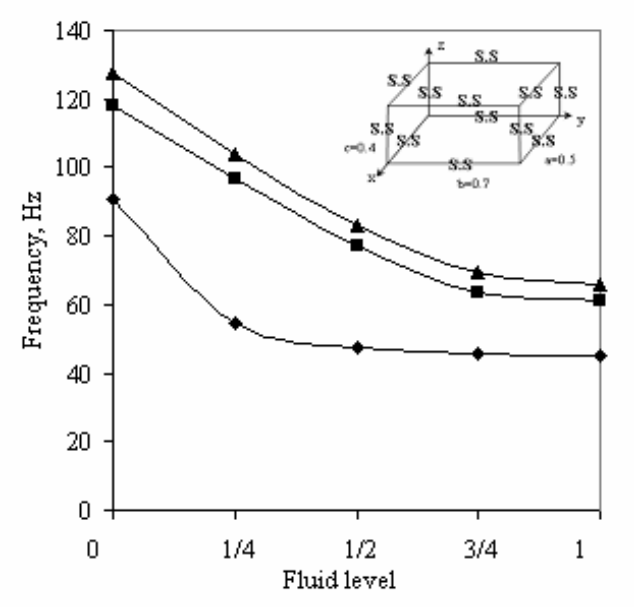

Fig. 12: Variation of frequencies of a simply supported reservoir at all edges versus fluid level variations

As we expected, the natural frequency of structure in vicinity of fluid decreases. It has been observed from Figs. 6-12 that the frequencies of fluid-filled reservoir have substantially decreased in comparison with reservoir in vacuo. For the first frequency about 50 % reduction has been obtained. We observe different behaviors of natural frequencies depending on boundary conditions. It is observed in Figs. 10 and 12 that the natural frequencies decrease as fractional filling increases and in the range of 3/4 to 1, frequencies are almost constant. For the 2nd and 3rd frequencies, substantial reduction has been observed over the range of 0 to 3/4, whereas in Fig. 10 for the 1st frequency the rate of change over fluid level variation is not appreciable. In Fig.12, 1st frequency decreases rapidly in the range of 0 to 1/4 and afterward it is almost unchangeable.

4.3. Submerged blade

In order to demonstrate the applicability of the proposed method a clamped-free blade in vacuo as well as a submerged blade in fluid is investigated. The blade has the same material properties as the reservoir and its length, width and thickness are 20, 10 and 1 cm, respectively. The blade has been discretized to 40×20 elements and water has been used as fluid. The heights of fluid over and under an arbitrary element and origin of blade are h_1, h_2, h_{o1} and h_{o2}, respectively as shown in Fig.13.

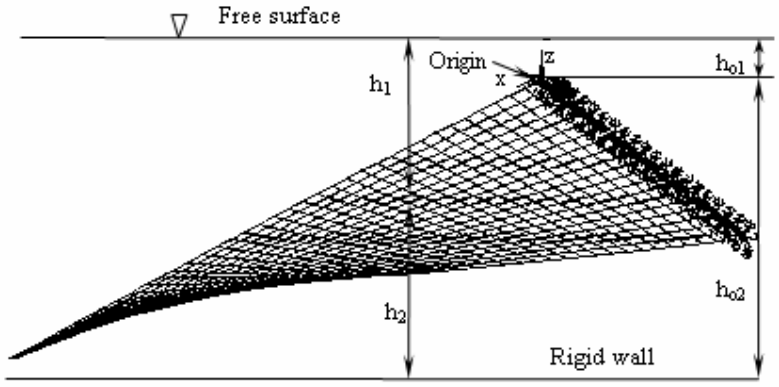

Fig. 13: Submerged blade

Natural frequencies of the blade in vacuo have been demonstrated in table. 5. The level of fluid over and under the blade as well as the boundary conditions of fluid (free surface, rigid wall or elastic object) affect the behavior of blade until a certain height of fluid. In order to clarify this phenomenon, variations of fluid height over and under blade are investigated individually. We observed when the blade is completely submerged in the fluid with a sufficiently large height under and over the blade; fluid level does not influence the frequency.

Table.5: Comparison of natural frequencies of a clamped-free blade (10×20×1cm) in vacuo

Natural Frequency (Hz)		
ANSYS	Present element	Discrepancy
212.47	236.2	0.100465707
1045.8	1087	0.037902484
1050.5	1123	0.064559216
2166.5	2148	0.008612663
3207.9	3251	0.013257459
3533.6	3581	0.013236526
5570.4	5642	0.012690535
5834.9	5883	0.008176101

Structures with different boundary conditions behave differently in vicinity of fluid. The level of fluid at which the frequency stops changing, varies from one structure to another. Consider a blade completely submerged in fluid as shown in Fig.13. Free surface and rigid wall are considered as boundary conditions. The free surface behavior is obtained by Eq. (64) and the rigid wall behavior is expressed by:

$$\frac{\partial \phi}{\partial z}\Big|_{z=-h-h_2} = 0 \tag{76}$$

The total pressure applying on each element is obtained by introducing these boundary conditions into Eqs. (61) and (62):

$$P_{total} = -\rho_f \left(\frac{1 - e^{2\mu h_1}}{\mu(1 + e^{2\mu h_1})} - \frac{1 + e^{2\mu h_2}}{\mu(e^{2\mu h_2} - 1)} \right) \frac{\partial^2 W}{\partial t^2} \tag{77}$$

$$Z_f = \frac{1 - e^{2\mu h_1}}{\mu(1 + e^{2\mu h_1})} - \frac{1 + e^{2\mu h_2}}{\mu(e^{2\mu h_2} - 1)} \tag{78}$$

Variations of the first few frequencies in function of fluid height variations over and under blade have been demonstrated in Figs.14 a-b and Figs.15 a-b, respectively. When the height of fluid over the blade increases, the frequency decreases. However, this reduction ceases when the height-length ratio reaches 50%. On the other hand, when the height of fluid under the blade increases, the frequency increases as well, but this increase stops when fluid level reaches 50% of length of blade. Because of geometry restrictions, height over and under the mentioned blade could not be reduced less than 16% in order to be completely submerged in fluid. Variation of frequencies as a function of simultaneous changes in h_{o1} and h_{o2} has been shown in Fig. 16. We observe that the frequency decreases rapidly during an increase of a height to length ratio from zero to 0.16 and then it increases slightly and afterward at $h_o / L \geq 0.3$, the augmentation ceases.

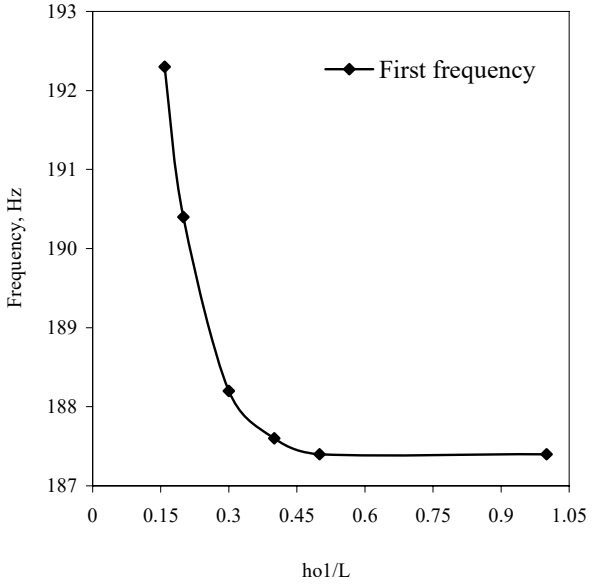

Fig 14-a: Variation of 1st frequency as a function of h_{o1} variations at sufficiently large h_{o2}

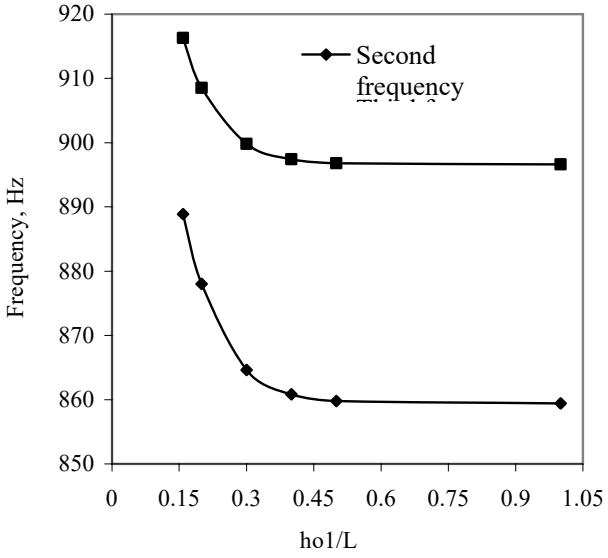

Fig 14-b: Variation of 2nd and 3rd frequencies as a function of h_{o1} variations at sufficiently large h_{o2}

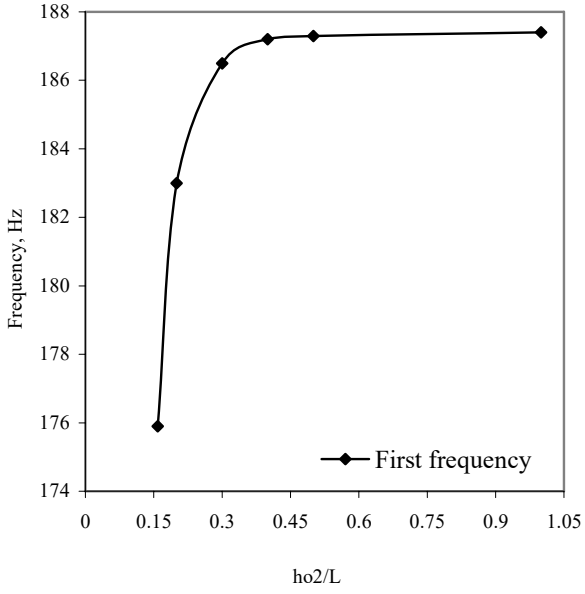

Fig 15-a: Variation of 1st frequency as a function of h_{o2} variations at sufficiently large h_{o1}

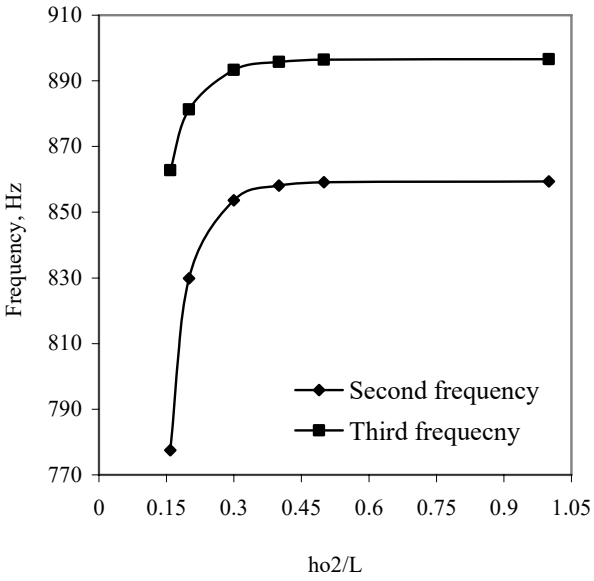

Fig 15-b: Variation of 2nd and 3rd frequencies as a function of h_{o2} variations at sufficiently large h_{o1}

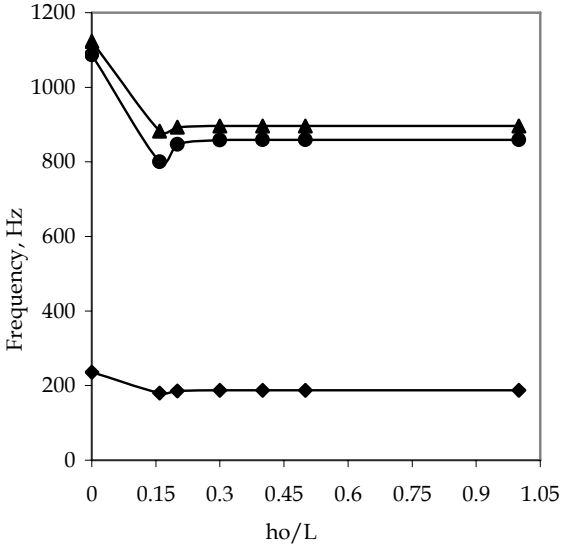

Fig 16: Variation of frequency as a function of simultaneous changes in h_o, where $h_o=h_{o1}=h_{o2}$

5. Conclusion

A method of analysis is presented for the dynamic behavior of elastic structures partially or completely filled with or submerged in stationary fluid. The method has demonstrated the versatility of the method developed through a rectangular flat shell element. This method is enable to predict the natural frequencies of three-dimensional thin structure containing or/and submerged in fluid. The shape functions developed in this method are calculated directly on the basis of the equations of motion and consequently the stiffness and mass matrices are determined by exact analytical integration of the equilibrium equations instead of the usually used and more arbitrarily interpolation polynomials as ANSYS or ABAQUS does. This work covers a variety of fluid-structure interaction issues, i.e. fluid random turbulence; flowing fluid and etc. All these aspects are not taken into account in one computer code, such as ABAQUS or any other FEM, therefore the necessity of this hybrid element, which is obtained by combination of finite element method and thin shell theory, arises to precisely calculate dynamic response of fluid-structure system. This work will be performed to investigate the natural frequencies of “n” blades in vacuo, submerged and/or subjected to a turbulent flow.

References

[1] Lindholm, U. S. et al, Elastic vibration characteristics of cantilever plates in water, *Journal of Ship Research*, 9, 1965.

[2] Fu, Y. and Price, W. G. Interaction between a partially or totally immersed vibrating cantilever plate and the surrounding fluid. *Journal of Sound and vibration*, 118, 495-513, 1987.

[3] Soedel, S. M. and Soedel, W. On the free and forced vibration of a plate supporting a freely sloshing surface liquid. *Journal of Sound and Vibration*, 171(2), 159-171, 1994.

[4] Amabili, M., Effect of finite fluid depth on the hydroelastic vibrations of circular and annular plates, *Journal of Sound and Vibration*, 193, 1996.

[5] Haddara, M. R. and Cao, S., Study of the dynamic response of submerged rectangular flat plates, *Marine Structures*, 9, 1996.

[6] Païdoussis, M. P., Flow-induced instabilities of cylindrical structures, *Applied Mechanics Review*, 40, 1987.

[7] Païdoussis, M. P. Fluid-Structure Interactions: Slender Structures and Axial Flow, Vol. I, Academic Press, London, 1998.

[8] Païdoussis, M. P. Fluid-Structure Interactions: Slender Structures and Axial Flow, Vol. II, Elsevier, 2004.

[9] Lakis, A. A. and Païdoussis, M. P., Free vibration of cylindrical shells partially filled with liquid, *Journal of Sound and Vibration*, 19, 1971.

[10] Lakis, A. A. and Païdoussis, M. P., Dynamic analysis of axially non-uniform thin cylindrical shells, *Journal of Mechanical Engineering Science*, 14, 1972.

[11] Toorani, M. H. and Lakis, A. A., Dynamics behavior of axisymmetric and beam-like anisotropic cylindrical shells conveying fluid, *Journal of Sound and Vibration*, 259, 2003.

[12] Toorani, M. H. and Lakis, A. A. Flow-induced vibration of anisotropic cylindrical shells 2002 ASME International Mechanical Engineering Congress and Exposition, Nov 17-22 2002, American Society of Mechanical Engineers, New York, NY 10016-5990, United States, New Orleans, LA, United States, 1251-1260, 2002.

[13] Toorani, M. H. and Lakis, A. A. Dynamic analysis of anisotropic cylindrical shells containing flowing fluid 2001 ASME Pressure Vessels and Piping Conference, Jul 22-26 2001, American Society of Mechanical Engineers, New York, NY 10016-5990, United States, Atlanta, GA, United States, 165-174, 2001.

[14] Lakis, A. A. et al, Non-linear dynamic analysis of cylindrical shells subjected to a flowing fluid, *American Society of Mechanical Engineers, Applied Mechanics Division, AMD*, 238, 2000.

[15] Toorani, M. H. and Lakis, A. A., Shear deformation in dynamic analysis of anisotropic laminated open cylindrical shells filled with or subjected to a flowing fluid, *Computer Methods in Applied Mechanics and Engineering*, 190, 2001.

[16] Lakis, A. A. et al, Dynamic analysis of anisotropic fluid-filled conical shells, *Journal of Fluid and Structure*, 6, 1992.

[17] Lakis, A. A. et al, Analysis of axially non-uniform thin spherical shells, *International*

Symposium on STRUCOPT-COMPUMAT, Paris, France, 1989.

[18] Selmane, A. and Lakis, A. A., Vibration Analysis of Anisotropic Open Cylindrical Shells Subjected to a Flowing Fluid, *Journal of Fluids and Structures*, 11, 1997.

[19] Lakis, A. A. and Neagu, S., Free surface effects on the dynamics of cylindrical shells partially filled with liquid, *Journal of Sound and Vibration*, 207, 1997.

[20] Jae Kwan Kim et al, Dynamic response of rectangular flexible fluid containers, *Journal of Engineering Mechanics*, 122, 1996.

[21] Kim, M. C. and Lee, S. S. Hydroelastic analysis of a rectangular tank The Aerospace Corporation, El Segundo California,

[22] Kyeong-Hoon Jeong et al, Hydroelastic vibration of two identical rectangular plates, *Journal of Sound and Vibration*, 272, 2004.

[23] Bauer, H. F. and Eidel, W., Hydroelastic vibrations in a two-dimensional rectangular container filled with frictionless liquid and a partly elastically covered free surface, *Journal of Fluids and Structures*, 19, 2004.

[24] Kerboua, Y., Lakis, A. A., Thomas, M., and Marcouiller, L. Analyse dynamique des systèmes de plaques en interaction avec un fluide et applications. École Polytechnique de Montreal, EPM-RT-2006-01, 2006.

[25] Charbonneau, E. and Lakis, A. A., Semi-analytical shape functions in the finite element analysis of rectangular plates, *Journal of Sound and Vibration*, 242, 2001.

[26] Lamb, H. Hydrodynamics, Dover Publications, New York, NY, United States, 1945.

Nomenclature

x_e, y_e	Dimensions of element in x and y directions, respectively
A, B	Plate's length and width in x and y directions, respectively
P_{ij}	Terms of elasticity matrix
P	Pressure imposing from fluid on the shell
U, V	Displacements of the shell reference surface in the x and y directions, respectively
W	Normal displacement of the shell reference surface
g	Gravitational acceleration
h	Shell thickness
h_1	Height of fluid over the shell
h_2	Height of fluid under the shell
ρ_s	Density of the shell material
ρ_f	Fluid density
ν	Poisson's coefficient
E	Modulus of elasticity
$\phi(x, y, z, t)$	Velocity potential function
$\{\delta_i\}$	Nodal displacement vector
$\{\varepsilon\}$	Strain vector
$\{\sigma\}$	Stress vector
$[K]_e$	Stiffness matrix of an element
$[K]_{Global}$	Global stiffness matrix
$[M]_e$	Mass matrix of an element

$[M]_{Global}$ Global mass matrix

$[M_f]$ Fluid mass matrix

$[N]$ Shape function matrix

$[P]$ Elasticity matrix

$[T]$ Transformation matrix

L'École Polytechnique se spécialise dans la formation d'ingénieurs et la recherche en ingénierie depuis 1873

École Polytechnique de Montréal

École affiliée à l'Université de Montréal

Campus de l'Université de Montréal
C.P. 6079, succ. Centre-ville
Montréal (Québec)
Canada H3C 3A7

www.polymtl.ca

ÉCOLE
POLYTECHNIQUE
MONTRÉAL